

Random Ising Spins in Two Dimensions - A Flat Space Realization of the KPZ Exponents

Marco Vekić

Institute for Theoretical Physics, University of California Santa Barbara, CA 93106

Shao Liu

Department of Physics, University of California Irvine, CA 92717

Herbert W. Hamber

Theory Division, CERN, CH-1211 Genève 23, Switzerland

(November 21, 2018)

Abstract

A model describing Ising spins with short range interactions moving randomly in a plane is considered. In the presence of a hard core repulsion, which prevents the Ising spins from overlapping, the model is analogous to a dynamically triangulated Ising model with spins constrained to move on a flat surface. As a function of coupling strength and hard core repulsion the model exhibits multicritical behavior, with first and second order transition lines terminating at a tricritical point. The thermal and magnetic exponents computed at the tricritical point are consistent with the KPZ values associated with Ising spins, and with the exact two-matrix model solution of the random Ising model, introduced previously to describe the effects of fluctuating geometries.

I. INTRODUCTION

Following the exact solution of the Ising model on a random surface by matrix model methods [1], there has been growing interest in the properties of random Ising spins coupled to two-dimensional gravity. More recently, work based on both series expansions [2,3] and numerical simulations [4,5] has verified and extended the original results. It is characteristic of these Ising models that the spins are allowed to move at random on a discretized version of a fluid surface. In a specific implementation of the model, Ising spins are placed at the vertices of a lattice built out of equilateral triangles, and the lattice geometry is then allowed to fluctuate by varying the local coordination number through a “link flip” operation which varies the local connectivity [4]. Remarkably, the same critical exponents have also been found using consistency conditions derived from conformal field theory for central charge $c = \frac{1}{2}$ [6], which should again apply to Ising spins. It is generally believed that the new values for the Ising critical exponents are due to the random fluctuations of the surface in which the spins are embedded, and therefore intimately tied to the intrinsic fractal properties of fluctuating geometries. It came therefore as a surprise that non-random Ising spins, placed on a randomly fluctuating geometry but with fixed spin coordination number, exhibited the same critical behavior as in flat space, without any observed “gravitational” shift of the exponents [7].

The natural question is then to what extent the values of the critical Ising exponents found by KPZ for $c = \frac{1}{2}$ and in the matrix model solution ($\alpha = -1$, $\beta = 1/2$, $\gamma = 2$, $\eta = 2/3$, $\nu = 3/2$ [1,6]) are due to the *annealed* randomness of the lattice, and to what extent they are due to the physical presence of a fluctuating background metric. The most straightforward way to answer this question is to investigate the critical properties of annealed random Ising spins, with interactions designed to mimic as closely as possible the dynamical triangulation model, but placed in flat two-dimensional space. It is well known that for a *quenched* random lattice the critical exponents are the same as on a regular lattice [8], as expected on the basis of universality, even though in two dimensions the Harris criterion (which applies to

quenched impurities only) does not give a clear prediction, since the specific heat exponent vanishes, $\alpha = 0$, for Onsager's solution.

In this paper we present some detailed results concerning the exponents of such a model in order to complete the discussion presented in a recent publication [9].

II. FORMULATION OF THE MODEL

In a square d -dimensional box of sides L with periodic boundary conditions we introduce a set of $N = L^d$ Ising spins $S_i = \pm 1$ with coordinates x_i^a , $i = 1 \dots N$, $a = 1 \dots d$, and average density $\rho = N/L^d = 1$. Both the spins and the coordinates will be considered as dynamical variables in this model. Interactions between the spins are determined by

$$I[x, S] = - \sum_{i < j} J_{ij}(x_i, x_j) W_{ij} S_i S_j - h \sum_i W_i S_i \quad , \quad (1)$$

with ferromagnetic coupling

$$J_{ij}(x_i, x_j) = \begin{cases} 0 & \text{if } |x_i - x_j| > R \\ J & \text{if } r < |x_i - x_j| < R \end{cases} \quad , \quad (2)$$

and infinite energy for $|x_i - x_j| < r$, giving therefore a hard core repulsion radius equal to $r/2$. As will be discussed further below, the hard core repulsive interaction is necessary for obtaining a non-trivial phase diagram, and mimics the interaction found in the dynamical triangulation model, where the minimum distance between any two spins is restricted to be one lattice spacing. For $r \rightarrow 0$, $J_{ij} = J[1 - \theta(|x_i - x_j| - R)]$.

The weights W_{ij} and W_i appearing in Eq. (1) could in principle contain geometric factors associated with the random lattice subtended by the points, and involve quantities such as the areas of the triangles associated with the vertices, as well as the lengths of the edges connecting the sites. In the following we will consider only the simplest case of unit weights, $W_{ij} = W_i = 1$. On the basis of universality of critical behavior one would expect that the results should not be too sensitive to such a specific choice, which only alters the short distance details of the model, and should not affect the exponents.

The full partition function for coordinates and spins is then written as

$$Z = \prod_{i=1}^N \sum_{S_i=\pm 1} \left(\prod_{a=1}^d \int_0^L dx_i^a \right) \exp(-I[x, S]) \quad . \quad (3)$$

In the following we will only consider the two-dimensional case, $d = 2$, for which specific predictions are available from the work of KPZ and the matrix model solution.

It should be clear that if the interaction range R is of order one, then, for sufficiently large hard core repulsion, $r \rightarrow \sqrt{5}/2 < R$, the spins will tend to lock in into an almost regular triangular lattice. As will be shown below, in practice this crossover happens already for quite small values of r . The critical behavior is then the one expected for the regular Ising model in two dimensions, namely a continuous second order phase transition with the Onsager exponents. Indeed for the Ising model on a triangular lattice it is known that $J_c = \frac{1}{2}\sqrt{3}\ln 3 = 0.9514\dots$. On the other hand if the hard core repulsion is very small, then for sufficiently low temperatures the spins will tend to form tight ordered clusters, in which each spin interacts with a large number of neighbors. As will be shown below, this clustering transition is rather sudden and strongly first order. Furthermore, where the two transition lines meet inside the phase diagram one would expect to find a tricritical point.

In order to investigate these issues further, we have chosen to study the above system by numerical simulation, with both the spins and the coordinates updated by a standard Monte Carlo method. The computation of thermodynamic averages is quite time consuming in this model, since any spin can in principle interact with any other spin as long as they get sufficiently close together. As a consequence, a sweep through the lattice requires a number of order N^2 operations, which makes it increasingly difficult to study larger and larger lattices. In order to extend our study to even larger lattices, we have applied a binning procedure in such a way that the time for the updating of a given configuration grows as zN , where z is the average coordination number of the lattice, instead of N^2 . This binning procedure consists of dividing the system in cells of unit length, and keeping track of the spins in each cell. Since all the moves are local, and spins can only move from a given cell to the neighboring ones, we only need to consider the spins in a given cell and its neighbors at

each updating step. This procedure is very effective when the average coordination number is relatively small ($J < J_c$ and r large), however, if $z \sim N$ the updating time grows again as N^2 .

In this paper we will not address in detail the problem of critical slowing down, however an additional possibility for the future could be to implement some sort of cluster updating algorithm [11]. On the other hand, we should add that we have not found any anomalous behavior as far as the autocorrelation times are concerned, which remain quite comparable to the pure Ising case.

There are a number of local averages and fluctuations which can be determined and used to compute the critical exponents. In the course of the simulation the spontaneous magnetization per spin

$$M = \frac{1}{N} \frac{\partial}{\partial h} \ln Z|_{h=0} = \frac{1}{N} \langle |\sum_i S_i| \rangle \quad , \quad (4)$$

was measured (here the averages involve both the x and S variables, $\langle \rangle \equiv \langle \rangle_{x,S}$), as well as the zero field susceptibility

$$\chi = \frac{1}{N} \frac{\partial^2}{\partial h^2} \ln Z|_{h=0} = \frac{1}{N} \langle \sum_{ij} S_i S_j \rangle - \frac{1}{N} \langle |\sum_i S_i| \rangle^2 \quad . \quad (5)$$

It is customary to use the absolute value on the r.h.s., since on a finite lattice the spontaneous magnetization, defined without the absolute value, vanishes identically even at low temperatures. In addition, in order to determine the latent heat and the specific heat exponent, we have computed the average Ising energy per spin defined here as

$$E = -\frac{1}{N} \frac{\partial}{\partial J} \ln Z|_{h=0} = -\frac{1}{JN} \langle \sum_{i<j} J_{ij}(x_i, x_j) W_{ij} S_i S_j \rangle \quad , \quad (6)$$

and its fluctuation,

$$C = \frac{1}{N} \frac{\partial^2}{\partial J^2} \ln Z|_{h=0} \quad . \quad (7)$$

Some additional quantities we have used in the course of this work will be defined later.

III. RESULTS AND ANALYSIS

In the simulations we have investigated lattice sizes varying from $5^2 = 25$ sites to $30^2 = 900$ sites. The length of our runs varies in the critical region ($J \sim J_c$) between 2M sweeps on the smaller lattices and 200k sweeps on the largest lattices. A standard binning procedure then leads to the errors reported in the figures.

As it stands, the model contains three coupling parameters, the ferromagnetic coupling J , the interaction range R and the hard core repulsion parameter r . We have fixed $R = 1$; comparable choices should not change the universality class. As we alluded previously, for small r we find that the system undergoes a sharp first order transition, between the disordered phase and a phase in which all spins form a few very tight magnetized clusters, in which the number of neighbors is of the order N . These clusters persist even for larger values of the hard core repulsion, r , but the number of interacting neighbors does not become as large as N in this case.

In Figs. 1 and 2 we show the existence of these clusters when the hard core repulsion is as large as $r = 0.4$. In Fig. 1 we observe ferromagnetic order in small domains even though we are below J_c . On the other hand, in Fig. 2, where we are above J_c , the system has practically clustered into a single ferromagnetic domain. For sufficiently large r , the transition is Ising-like, between ordered and disordered, almost regular, Ising lattices (for our choice of range R , the transition appears to be very close to regular Ising-like for $r \approx 0.6$ and larger, see below). In Fig. 3 we show a particular configuration for $r = 0.98$ where the regular, almost triangular, lattice is clearly visible. In this case the average coordination number z is very close to 3, as expected for a regular triangular lattice. In Fig. 4 we show the average number of neighbors z for several values of r on a system with $N = 144$ spins. We find that for small values of r the coordination number increases very rapidly as we approach the critical point. On the other hand, for intermediate choices of r , z saturates to a smaller value. When $r = 0.6$, the coordination number saturates to a value of $z = 3.1$, which is already very close to the value on a regular triangular lattice ($z = 3$).

In Fig. 5 we plot the average energy per bond E_z as a function of J for several choices of the hard core repulsion r . The jump discontinuity, which is visible for small hard core repulsion r , indicates the existence of a first order transition. For larger values of r , the discontinuity is reduced and eventually vanishes. A determination of the discontinuity in the average energy of Fig. 5 at the critical coupling J_c shows that it gradually decreases as r is increased from zero. Fig. 6 shows a plot of the latent heat per bond Δ_z versus r at the transition point J_c . In general we do not expect the latent heat to vanish linearly at the endpoint, but our results seem to indicate a behavior quite close to linear. From the data we estimate that the latent heat vanishes at $r = 0.344(7)$, thus signaling the presence of a tricritical point at the end of the first order transition line. Beyond this point, the transition stays second order, as will be discussed further below. The phase transition line is shown in Fig. 15; for $r = 0$ we found on the largest lattices $J_c = 0.19(2)$, while for $r = 0.98$ we found $J_c = 0.93(3)$.

In Fig. 7 we plot the spin susceptibility as a function of J for several system sizes near the tricritical point, showing a growth of the peak with system size. To determine the critical exponents, we will resort to a finite-size scaling analysis. In the following we will be mostly concerned with the values for the critical exponents in the vicinity of the tricritical point. In the case of the spin susceptibility, from finite-size scaling, we expect a scaling form of the type

$$\chi(N, J) = N^{\gamma/2\nu} \bar{\chi}(N^{1/2\nu}|J - J_c|) \quad . \quad (8)$$

To recover the correct infinite volume result one needs $\bar{\chi}(x) \sim x^{-\gamma}$ for large arguments. Thus, in particular the peak in χ should scale like $N^{\gamma/2\nu}$ for sufficiently large N . In Fig. 8 we show the evolution of the computed peaks in χ as a function of $\ln N$.

Despite the fact that the lattices are quite small, as can be seen from the graph, a linear fit to the data at the tricritical point is rather good, with relatively small deviations from linearity, $\chi^2/d.o.f. \sim 10^{-4}$. Using least-squares one can estimate γ/ν . For $r = 0.35$ we find $\gamma/\nu = 1.32(3)$, which is much smaller than the exact regular Ising result $\gamma/\nu = 1.75$. From

scaling one then obtains the anomalous dimension exponent $\eta = 2 - \gamma/\nu = 0.68(3)$. To further gauge our errors, we have computed the same exponent for the regular Ising limit, for $r = 0.6$. In this case we indeed recover the Onsager value: we find on the same size lattices and using the same analysis method $\gamma/\nu = 1.72(4)$. We also note that the shift in the critical point on a finite lattice is expected to be determined by the correlation length exponent ν , namely $J_c(N) - J_c(\infty) \sim N^{-1/2\nu}$. This relationship can be used to estimate ν , but it is not very accurate. From a fit to the known values of $J_c(N)$ we obtain a first rough estimate $\nu = 1.3(2)$. A more precise determination of ν will be given later.

A similar finite-size scaling analysis can be performed for the magnetization, which is shown in Fig. 9 for several system sizes. Close to and above J_c we expect $M \sim (J - J_c)^\beta$. At the critical point on a finite lattice, as determined from the peak in the susceptibility (which incidentally is very close to the inflection point in the magnetization versus J), M should scale to zero as $M_N(J_c) \sim N^{\beta/2\nu}$. In Fig. 10 we show the magnetization M computed in this way for different size lattices. At the tricritical point we find $\beta/\nu = 0.31(4)$, which again clearly excludes the pure Ising exponent, $\beta/\nu = 0.125$. For the pure Ising limit ($r = 0.6$) we obtain $\beta/\nu = 0.13(7)$, which is close to the expected Onsager value.

The results for the Ising specific heat C at the tricritical point as a function of lattice size N are shown in Fig. 11. One expects the peak to grow as $C \sim N^{\alpha/2\nu}$, but the absence of any growth for the larger values of N implies that $\alpha/\nu < 0$ (a weak cusp in the specific heat). In general close to a critical point, the free energy can be decomposed into a regular and a singular part. In our case the singular part does not seem to be singular enough to emerge above the regular background, leading to an intrinsic uncertainty in the determination of an $\alpha < 0$, and which can only be overcome by determining still higher derivatives of the free energy with respect to the coupling J . In order to isolate the singular part of the specific heat we have therefore calculated dC/dJ from the expression

$$\frac{dC}{dJ} = N^2 \left[3\langle E \rangle \langle E^2 \rangle - \langle E^3 \rangle - 2\langle E \rangle^3 \right]. \quad (9)$$

In the infinite system dC/dJ should diverge according to

$$\frac{dC}{dJ} \sim |J - J_c|^{-(\alpha+1)}. \quad (10)$$

In particular, if $\alpha = -1$, dC/dJ should diverge logarithmically. In Fig. 12 we show the scaling of dC/dJ on a lattice with $N = 256$ spins according to Eq. (10). From the slope of the curve we determine the critical exponent to be $\alpha \approx -0.98(4)$. We have also tried to assume a logarithmic scaling behavior as shown in Fig. 13. It is clear that from the linear behavior of dC/dJ we can conclude that our results are completely consistent with an exponent of $\alpha = -1$. We attribute the small discrepancy between the results of Figs. 12 and 13 to the fact that we are not sufficiently close to J_c and that we are on a finite lattice with N sites. We have also performed a similar analysis for the fluctuation in the energy per bond (as opposed to the energy per site as defined previously). In this case we find close to the tricritical point $\alpha \approx -0.96(2)$.

In the *regular* Ising case one has in a finite volume a logarithmic divergence $C \sim \ln N$ (and $\alpha/2\nu = 0$), and we indeed see such a divergence clearly for $r = 0.6$, which corresponds to the almost regular triangular Ising case.

Another approach to obtaining α is to determine the correlation length exponent ν directly instead, and use scaling to relate it to $\alpha = 2 - 2\nu$. The exponent ν can be obtained in the following way. First one can improve on the estimate for J_c by considering the fourth-order cumulant [12]

$$U_N(J) = 1 - \frac{\langle m^4 \rangle}{3 \langle m^2 \rangle^2}, \quad (11)$$

where $m = \sum_i S_i/N$. It has the scaling form expected of a dimensionless quantity

$$U_N(J) = \bar{U}(N^{1/2\nu}|J - J_c|). \quad (12)$$

The curves $U_N(J)$, for different and sufficiently large values of N , should then intersect at a common point J_c , where the theory exhibits scale invariance, and U takes on the fixed point value U^* . In Fig. 14 we show the fourth-order cumulant as a function of J for $r = 0.35$ and for several lattice sizes. We have found that indeed the curves meet very close to a common

point, and from the intersection of the curves for $N = 25$ to 400 we estimate $J_c = 0.472(9)$, which is consistent with the estimate of the critical point derived from the location of the peak in the magnetic susceptibility. We also determine $U^* = 0.47(4)$, which should be compared to the pure Ising model estimate for the invariant charge $U^* \approx 0.613$ [13].

One can then estimate the correlation length exponent ν from the scaling of the slope of the cumulant at J_c . For two lattice sizes N, N' one computes the estimator

$$\nu_{eff}(N, N') = \frac{\ln[N'/N]}{2 \ln[U'_{N'}(J_c)/U'_N(J_c)]} \quad , \quad (13)$$

with $U'_N \equiv \partial U_N / \partial J$ defined by

$$U'_N = \frac{N}{3\langle m^2 \rangle^2} \left[\langle m^4 \rangle \langle E \rangle + \langle m^4 E \rangle - 2 \frac{\langle m^4 \rangle \langle m^2 E \rangle}{\langle m^2 \rangle} \right]. \quad (14)$$

Using values of N from systems with 256, 400, and 900 spins we estimate ν from Eq. (14) to be 1.46(8). Using the scaling relationship $\alpha = 2 - 2\nu$, we obtain an estimate for α which is again quite consistent with our previous estimate derived from dC/dJ .

In Table I we summarize our results, together with the exponents obtained for the two-matrix model [1] (and which are the same as the KPZ values [6]), for the Onsager solution of the square lattice Ising model, and for the tricritical Ising model in two dimensions [10]. As can be seen, the exponents are quite close to the matrix model values (the pure Ising exponents seem to be excluded by several standard deviations).

TABLES

TABLE I. Estimates of the critical exponents for the random two-dimensional Ising model, as obtained from finite-size scaling at the tricritical point.

	γ/ν	β/ν	α/ν	α	ν
This work	1.32(3)	0.31(4)	-0.65(4)	-0.98(4)	1.46(8)
Matrix model	1.333...	0.333...	-0.666...	-1.0	1.5
Onsager	1.75	0.125	0.0	0.0	1.0
Tricritical Ising	1.85	0.075	1.60	0.888...	0.555...

IV. CONCLUSIONS

In the previous sections we have presented some results for the exponents of a random Ising model in flat two-dimensional space. The model reproduces some of the features of a model for dynamically triangulated Ising spins, and in particular its random nature, but does not incorporate any effects due to curvature. Due to the non-local nature of the interactions of the spins, only relatively small systems have been considered so far, which is reflected in the still rather large uncertainties associated with the exponents. Still a rich phase diagram has emerged, with a tricritical point separating first from second order transition lines. The phase diagram we obtain is shown in Fig. 15. We have localized the tricritical point at $J_c = 0.471(5)$ and $r = 0.344(7)$. The thermal and magnetic exponents determined in the vicinity of the tricritical point (presented in Table I) have been found to be consistent, within errors, with the matrix model solution of the random Ising model and the KPZ values. Our results would therefore suggest that matrix model solutions can also be used to describe a class of annealed random systems in flat space.

One might wonder at this point if the spin system discussed in this paper can be found among the models in the FQS classification scheme [14] of two-dimensional conformally invariant field theories¹. Since the model is apparently not unitary (it contains short range repulsion and long range attraction terms), it should fall into the wider class of degenerate theories considered by BPZ [15]. The allowed scaling dimensions in these theories are given by the well-known Kac formula,

$$\Delta_{p,q} = \frac{1}{4} \left[(p\alpha_+ + q\alpha_-)^2 - (\alpha_+ + \alpha_-)^2 \right] \quad (15)$$

with p, q positive integers, and $\alpha_{\pm} = \alpha_0 \pm (1 + \alpha_0^2)^{1/2}$. α_0 is related to the conformal anomaly c of the theory by $c = 1 - 24\alpha_0^2$. Often the central charge is then written as $c = 1 - 6/m(m + 1)$. One of the difficulties in this approach is the identification of a

¹We thank Giorgio Parisi for suggesting to look into this aspect.

given realization of conformal symmetry with a particular universality class. The simplest possibility appears to be $m = 4/5$, corresponding to $m = r/(s - r)$ with $s = 9$ and $r = 4$. One then obtains for this choice the central charge $c = -19/6$, and $\alpha_0 = 5/12$, $\alpha_+ = 3/2$ and $\alpha_- = -2/3$. The matching scaling dimensions are then $\Delta_{1,4} = \Delta_{3,5} = 1/6$ (which gives $\eta = 2/3$), and $\Delta_{1,5} = \Delta_{3,4} = 2/3$ (which gives $\nu = 3/2$). Negative values of c are allowed in non-unitary theories. It would be of interest to compute the central charge directly in the random spin model and verify this assignment, using the methods described in Ref. [17].

We should mention in closing that the above values for s and r appear to be rather close to the ones associated with the Yang-Lee edge singularity, which describes the behavior of the magnetization in the Ising model in the presence of an imaginary external field, and for which Cardy [16] has suggested the identification $s = 5$ and $r = 2$, which yields $m = 2/3$ and $c = -22/5$. It is known that the Yang-Lee edge singularity also describes the critical properties of large branched dilute polymers and of the Ising model in a quenched random external field in $d + 2$ dimension [18].

Acknowledgements

One of us (H.W.H.) acknowledges useful discussions with G. Parisi during a visit at the University of Rome. We would also like to thank Martin Hasenbush for his comments related to this work. The numerical computations were performed on facilities provided by the National Center for Supercomputer Applications (NCSA), the San Diego Supercomputer Center (SDSC), the University of California at Irvine, and by the Texas National Research Laboratory Commission through grants RGFY9166 and RGFY9266.

REFERENCES

- [1] V.A. Kazakov, *Phys. Lett.* **A119** (1986) 140;
D.V. Boulatov and V.A. Kazakov, *Phys. Lett.* **B186** (1987) 379;
Z. Burda and J. Jurkiewicz, *Acta Physica Polonica* **20** (1989) 949.
- [2] E. Brezin and S. Hikami, *Phys. Lett.* **B283** (1992) 203;
Phys. Lett. **B295** (1992) 209; S. Hikami, *Phys. Lett.* **B305** (1993) 327;
E. Brezin, M.R. Douglas, V. Kazakov and S.H. Shenker, *Phys. Lett.* **B237** (1990) 43.
- [3] G.M. Cicuta, *Nucl. Phys. B* (Proc. Supp.) **5A** (1988) 54; and references therein.
- [4] P. Ben-Av, J. Kinar and S. Solomon, *Int. Jour. Mod. Phys.* **C3** (1992) 279.
- [5] J. Jurkiewicz, A. Krzywicki, B. Peterson and B. Söderberg, *Phys. Lett.* **B213** (1988) 511;
I.D. Aleinov, A.A. Migdal and V.V. Zmushko, *Mod. Phys. Lett.* **A5** (1990) 787;
C.F. Baille and D. A. Johnston, *Mod. Phys. Lett.* **A7** (1992) 1519;
S. Catterall, J. Kogut and R. Renken, *Phys. Rev.* **D45** (1992) 2957;
J. Ambjørn, B. Durhuus, T. Jonsson and G. Thorleifsson, NBI-HE-92-35 (1992);
J.-P. Kownacki and A. Krzywicki, preprint LPTHE-Orsay 94/11 (Jan 1994).
- [6] V.G. Knizhnik, A.M. Polyakov and A.B. Zamolodchikov, *Mod. Phys. Lett.* **A3** (1988) 819;
F. David, *Mod. Phys. Lett.* **A3** (1988) 1651;
J. Distler and H. Kawai, *Nucl. Phys.* **B321** (1989) 509.
- [7] M. Gross and H.W. Hamber, *Nucl. Phys.* **B364** (1991) 703.
- [8] D. Espriu, M. Gross, P. Rakow and J.F. Wheeler, *Nucl. Phys.* **B265** [FS15] (1986) 92;
W. Janke, M. Katoot and R. Villanova, *Phys. Lett.* **B315** (1993) 412.
- [9] M. Vekić, S. Liu, and H.W. Hamber, *Phys. Lett.* **B329** (1994) 444.

- [10] I.D. Lawrie and S. Sarbach, in *Phase Transitions and Critical Phenomena*, vol. 9, edited by C. Domb and J. Lebowitz (Academic Press, 1984); and references therein.
- [11] U. Wolff, *Phys. Rev. Lett.* **62** (1989) 361.
- [12] K. Binder, *Phys. Rev. Lett.* **47** (1981) 693; *Z. Phys.* **B43** (1981) 119.
- [13] K. Binder and D. Landau, *Surf. Sci.* **151** (1985) 409;
D. Heerman and A. Burkitt, *Physica A* **162** (1990) 210.
- [14] D. Friedan, Z. Qiu and S. Shenker, *Phys. Rev. Lett.* **52** (1984) 1575.
- [15] A.A. Belavin, A.M. Polyakov and A.B. Zamolodchikov, *J. Stat. Phys.* **34** (1984) 763.
- [16] J. Cardy, *Phys. Rev. Lett.* **54** (1985) 1354;
J. Cardy, in *Phase Transitions and Critical Phenomena*, vol. 11 (edited by C. Domb and J.L. Lebowitz, Academic Press, 1987).
- [17] H. Blöte, J. Cardy and M.P. Nightingale, *Phys. Rev. Lett.* **56** (1986) 742;
I. Affleck, *Phys. Rev. Lett.* **56** (1986) 746;
C. Itzykson, H. Saleur and J.-B. Zuber, *Europhys. Lett.* **2** (1986) 91.
- [18] G. Parisi and N. Surlas, *Phys. Rev. Lett.* **46** (1981) 871.

FIGURES

FIG. 1. A particular configuration of the system with $N = 400$ spins and $r = 0.4$ for $J = 0.35$. Spins with $S = \pm 1$ are indicated with empty and solid circles, respectively.

FIG. 2. A particular configuration of the system with $N = 400$ spins and $r = 0.4$ for $J = 0.65$. Spins with $S = \pm 1$ are indicated with empty and solid circles, respectively.

FIG. 3. A particular configuration of the system with $N = 400$ spins and $r = 0.98$ for $J = 0.25$. The hard core repulsion radius is shown as a circle around the spin. Spins with $S = \pm 1$ are indicated with empty and solid circles, respectively.

FIG. 4. The average number of neighbors z as a function of J on a lattice with $N = 144$ spins for several choices of the hard core repulsion r .

FIG. 5. The average energy per bond E_z as a function of J for several choices of the hard core repulsion r for a system with $N = 100$ sites.

FIG. 6. The latent heat per bond Δ_z along the first order transition line, plotted against the hard core repulsion parameter r . The tricritical point is located where the latent heat vanishes.

FIG. 7. The magnetic susceptibility χ versus J for fixed hard core repulsion parameter $r = 0.35$ and different system sizes.

FIG. 8. The peak in the magnetic susceptibility χ_{\max} versus the number of Ising spins N for choices of the hard core repulsion parameter corresponding to $r = 0.35$ and $r = 0.6$.

FIG. 9. The magnetization M versus J , for fixed hard core repulsion parameter $r = 0.35$ and different system sizes. The solid line is a spline through the data for $N = 144$.

FIG. 10. Finite size scaling of the magnetization at the inflection point M_{inf} versus the total number of Ising spins N for choices of the hard core repulsion parameter corresponding to $r = 0.35$ and $r = 0.6$.

FIG. 11. Plot of the specific heat C versus ferromagnetic coupling J at $r=0.35$, showing the absence of a growth in the peak with increasing lattice size (for the larger systems), in contrast to the behavior of the magnetic susceptibility. The errors (not shown) are smaller than the size of the symbols.

FIG. 12. The derivative of the specific heat dC/dJ as a function of $J_c - J$ on logarithmic axes for $N = 256$.

FIG. 13. The derivative of the specific heat dC/dJ as a function of $J_c - J$ on semi-logarithmic axes for $N = 256$.

FIG. 14. The Binder fourth-order cumulant U as a function of J for fixed hard-core repulsion $r = 0.35$ and on several lattices with N spins. The solid line is a spline through the data for $N = 144$.

FIG. 15. The phase diagram for the dynamical random Ising model on a two-dimensional flat surface. The tricritical point (denoted by the solid circle) separates the first order from the second order transition lines. The paramagnetic (PM) and ferromagnetic (FM) phases are also shown.

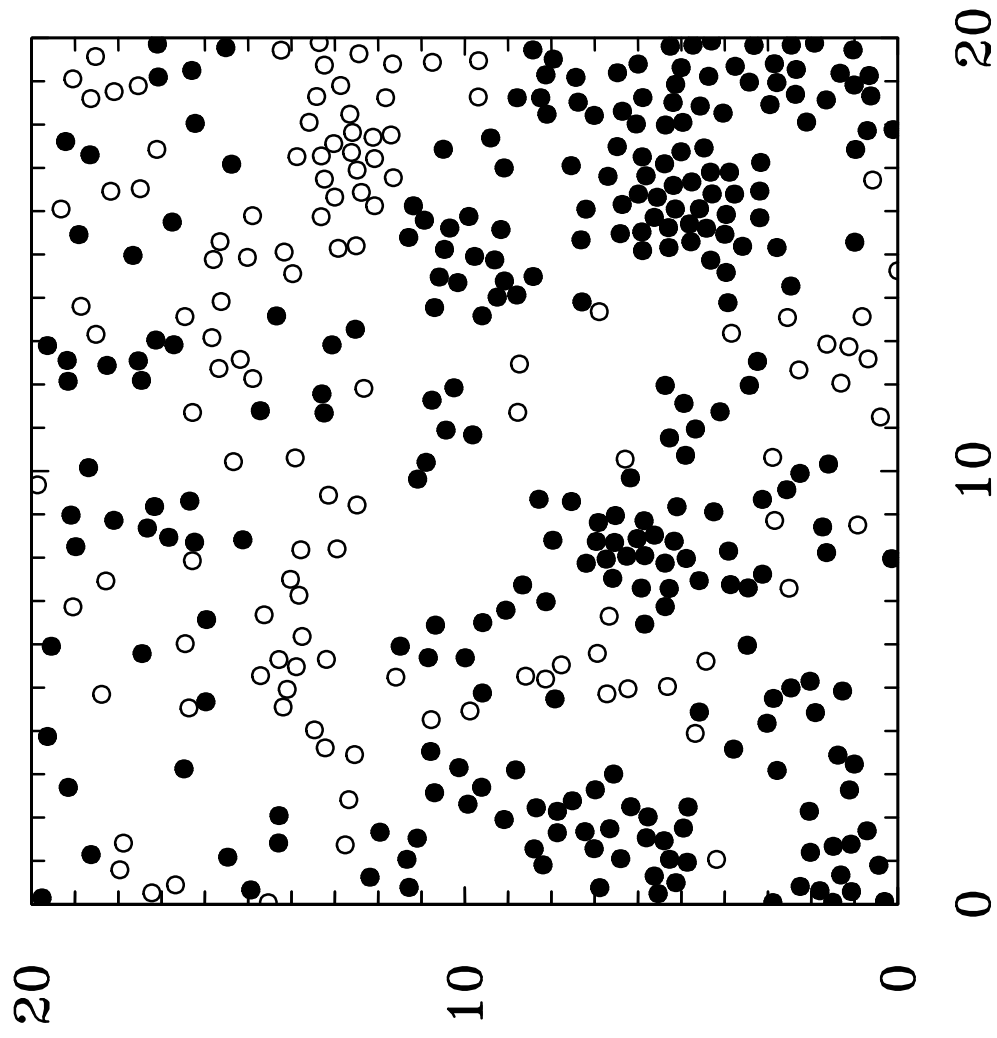


Fig.1

This figure "fig1-1.png" is available in "png" format from:

<http://arxiv.org/ps/hep-th/9407166v2>

This figure "fig2-1.png" is available in "png" format from:

<http://arxiv.org/ps/hep-th/9407166v2>

This figure "fig3-1.png" is available in "png" format from:

<http://arxiv.org/ps/hep-th/9407166v2>

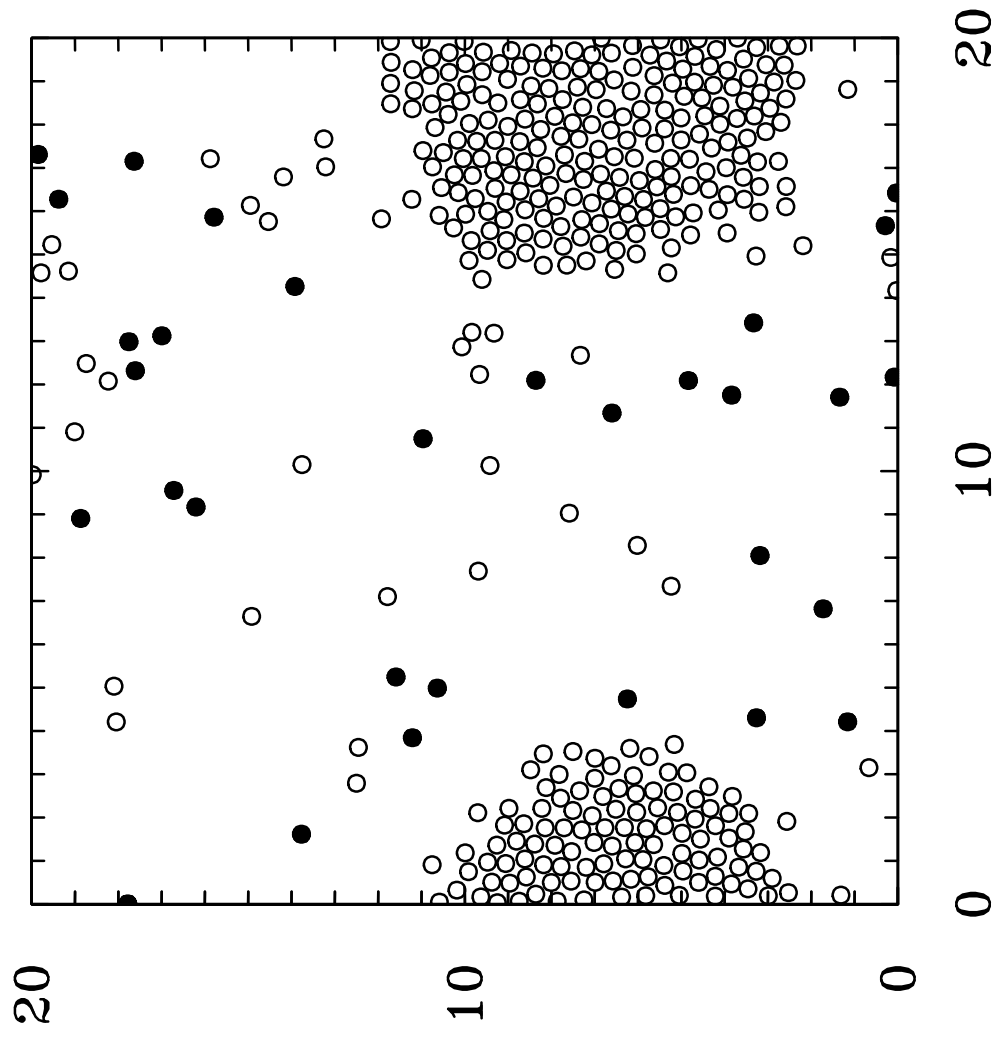


Fig.2

This figure "fig1-2.png" is available in "png" format from:

<http://arxiv.org/ps/hep-th/9407166v2>

This figure "fig2-2.png" is available in "png" format from:

<http://arxiv.org/ps/hep-th/9407166v2>

This figure "fig3-2.png" is available in "png" format from:

<http://arxiv.org/ps/hep-th/9407166v2>

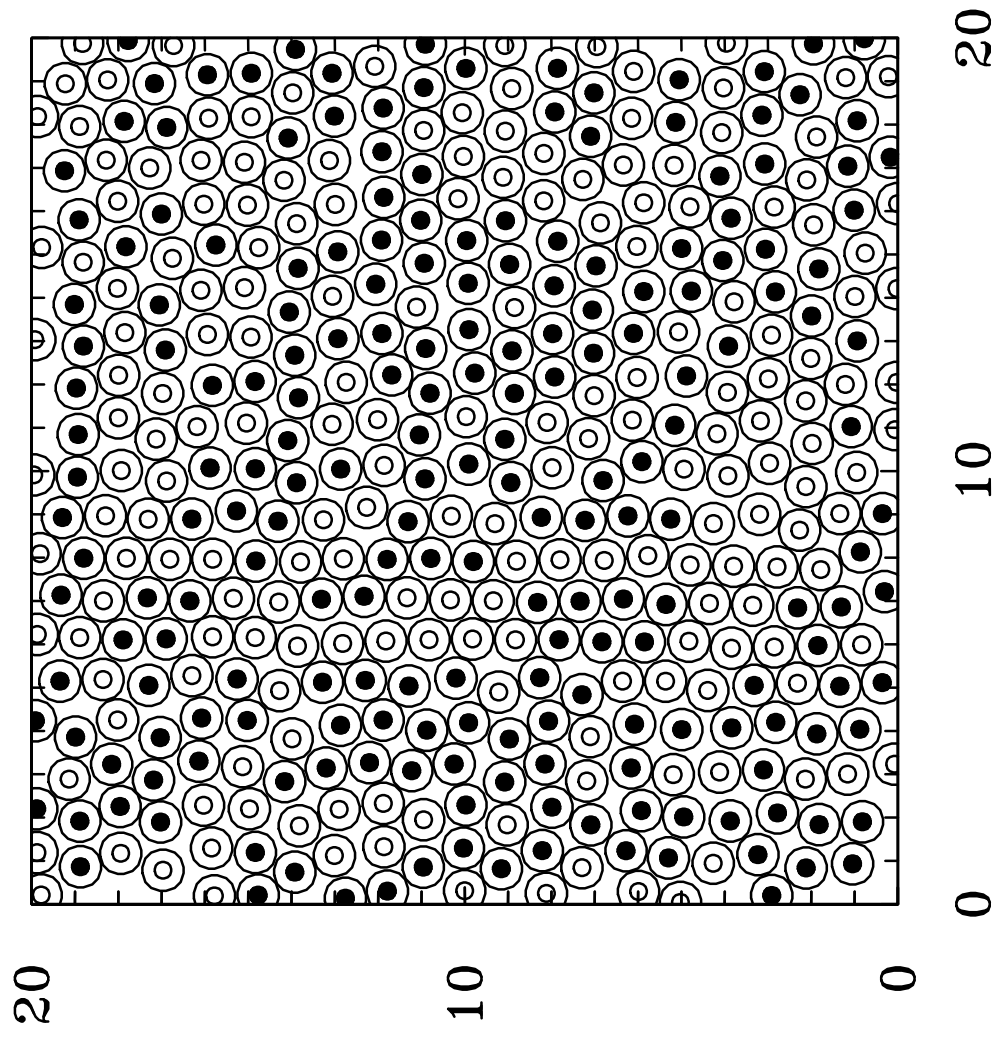


Fig.3

This figure "fig1-3.png" is available in "png" format from:

<http://arxiv.org/ps/hep-th/9407166v2>

This figure "fig2-3.png" is available in "png" format from:

<http://arxiv.org/ps/hep-th/9407166v2>

This figure "fig3-3.png" is available in "png" format from:

<http://arxiv.org/ps/hep-th/9407166v2>

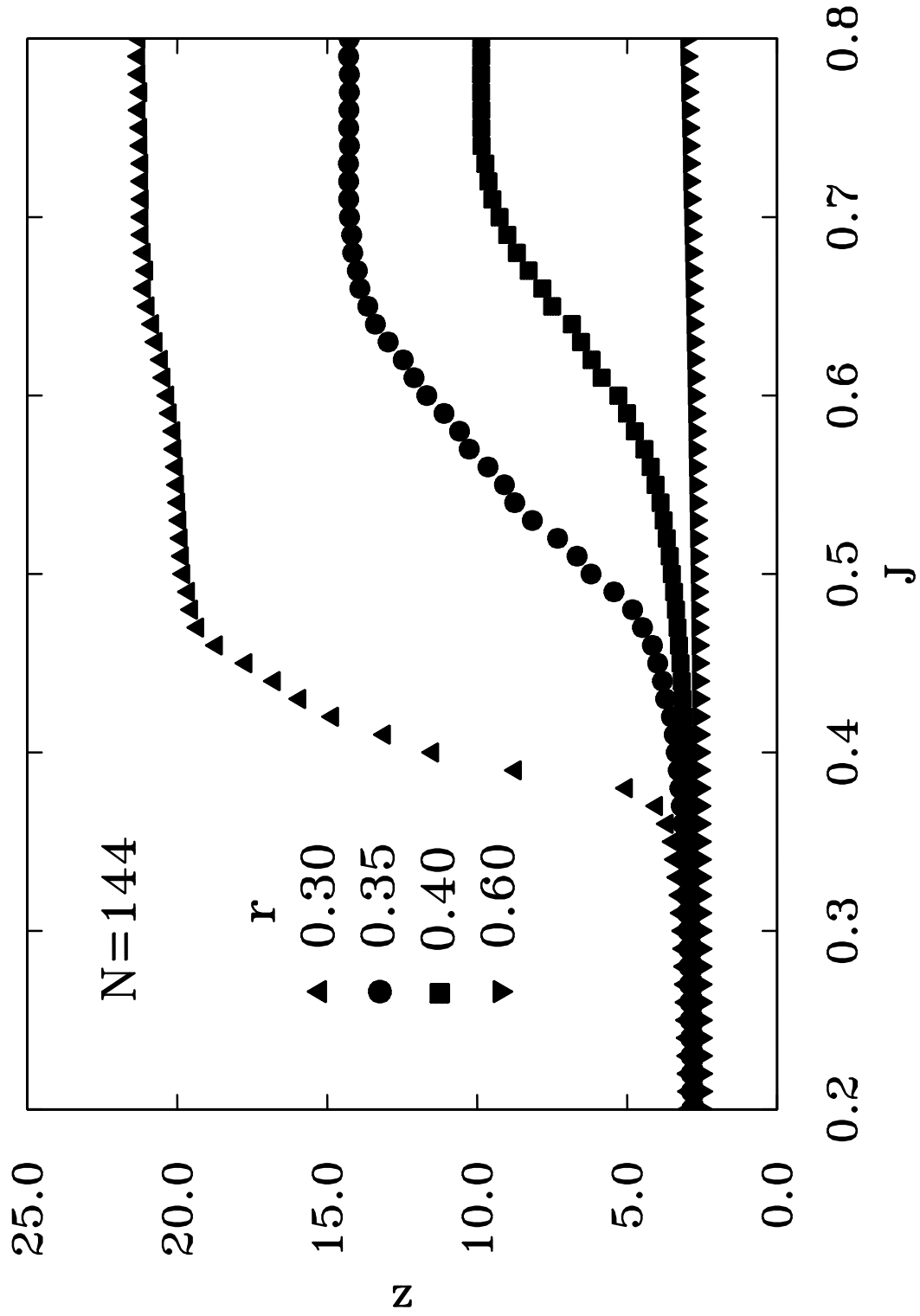


Fig.4

This figure "fig1-4.png" is available in "png" format from:

<http://arxiv.org/ps/hep-th/9407166v2>

This figure "fig2-4.png" is available in "png" format from:

<http://arxiv.org/ps/hep-th/9407166v2>

This figure "fig3-4.png" is available in "png" format from:

<http://arxiv.org/ps/hep-th/9407166v2>

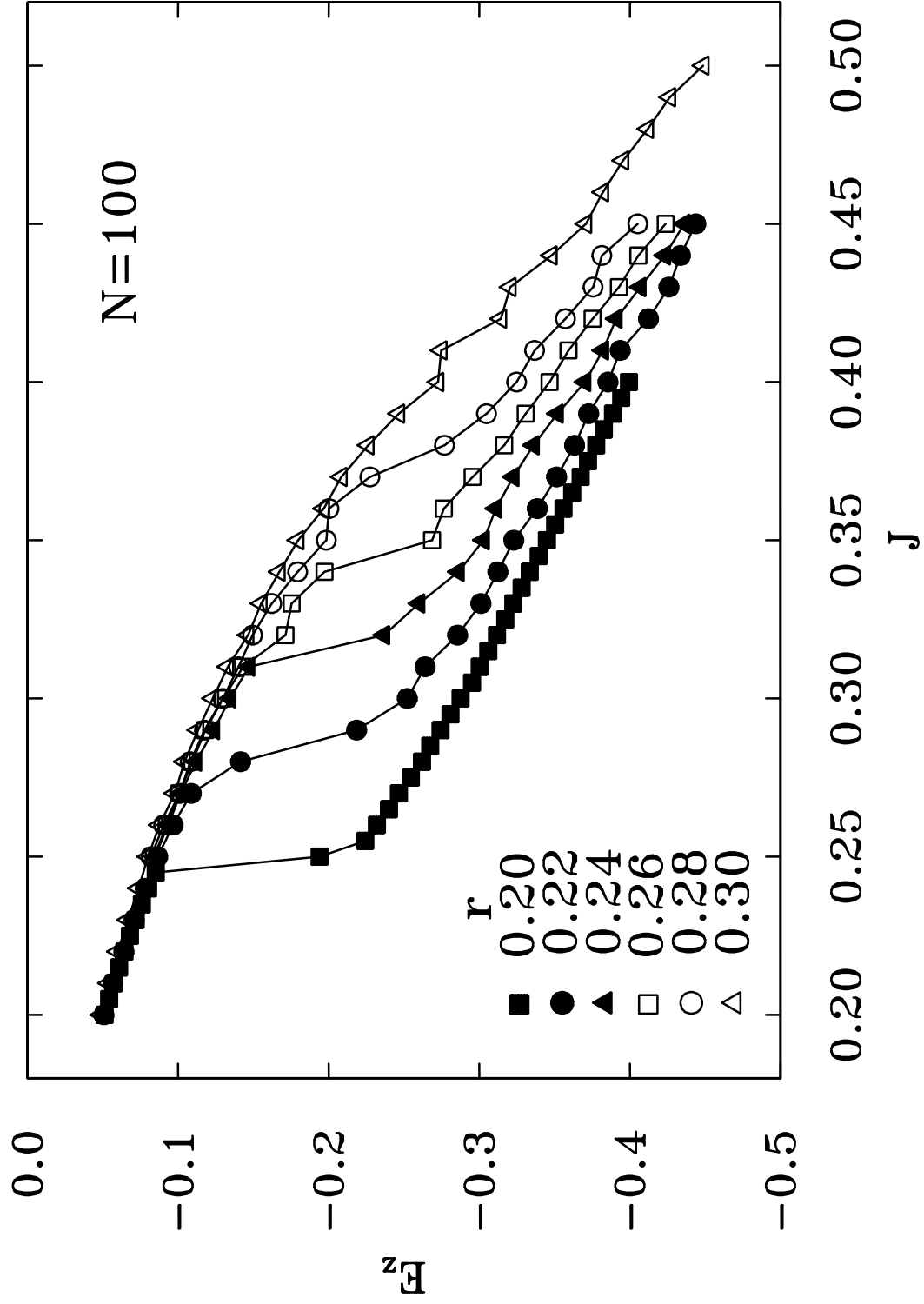


Fig.5

This figure "fig1-5.png" is available in "png" format from:

<http://arxiv.org/ps/hep-th/9407166v2>

This figure "fig2-5.png" is available in "png" format from:

<http://arxiv.org/ps/hep-th/9407166v2>

This figure "fig3-5.png" is available in "png" format from:

<http://arxiv.org/ps/hep-th/9407166v2>

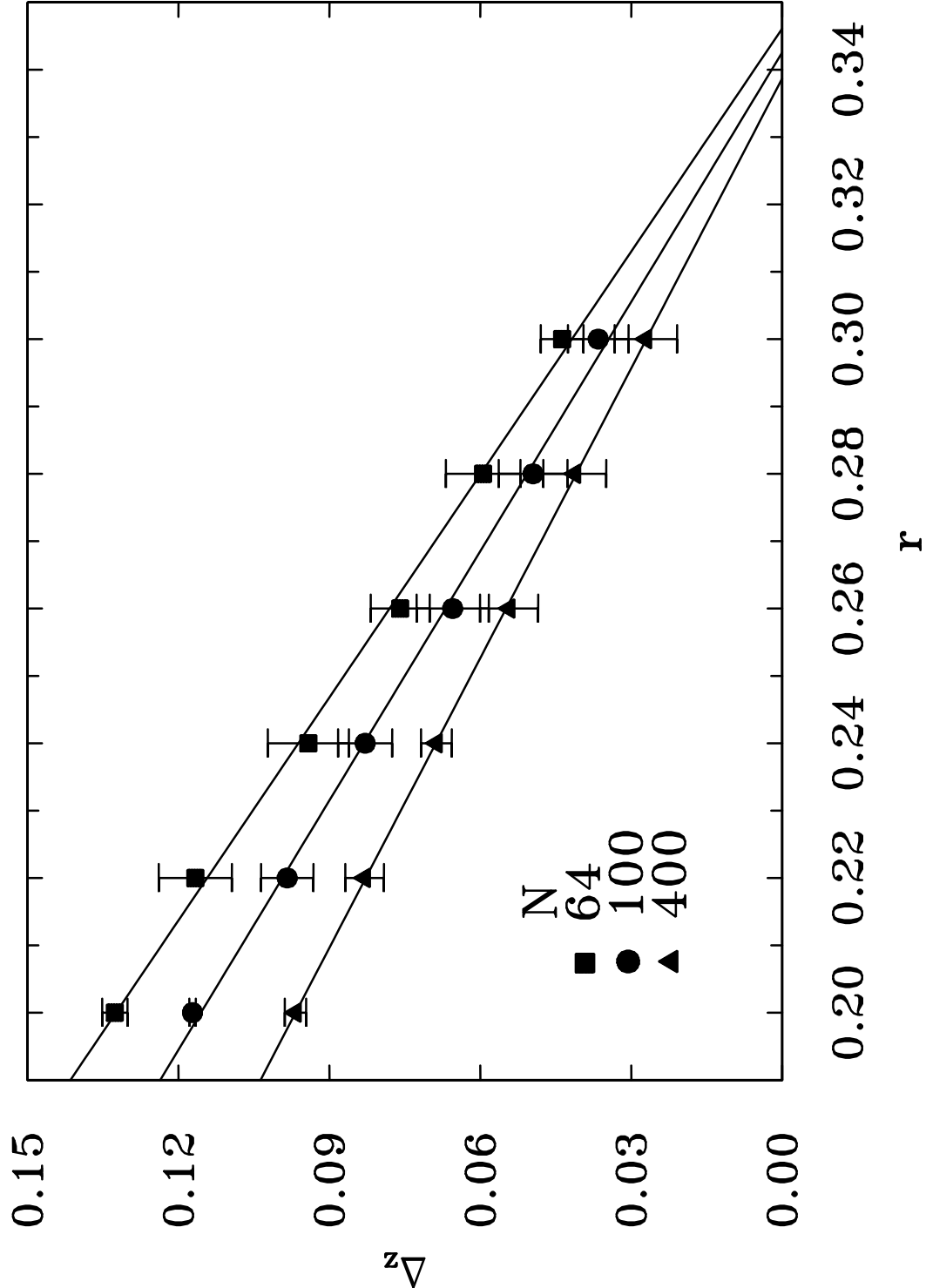


Fig.6

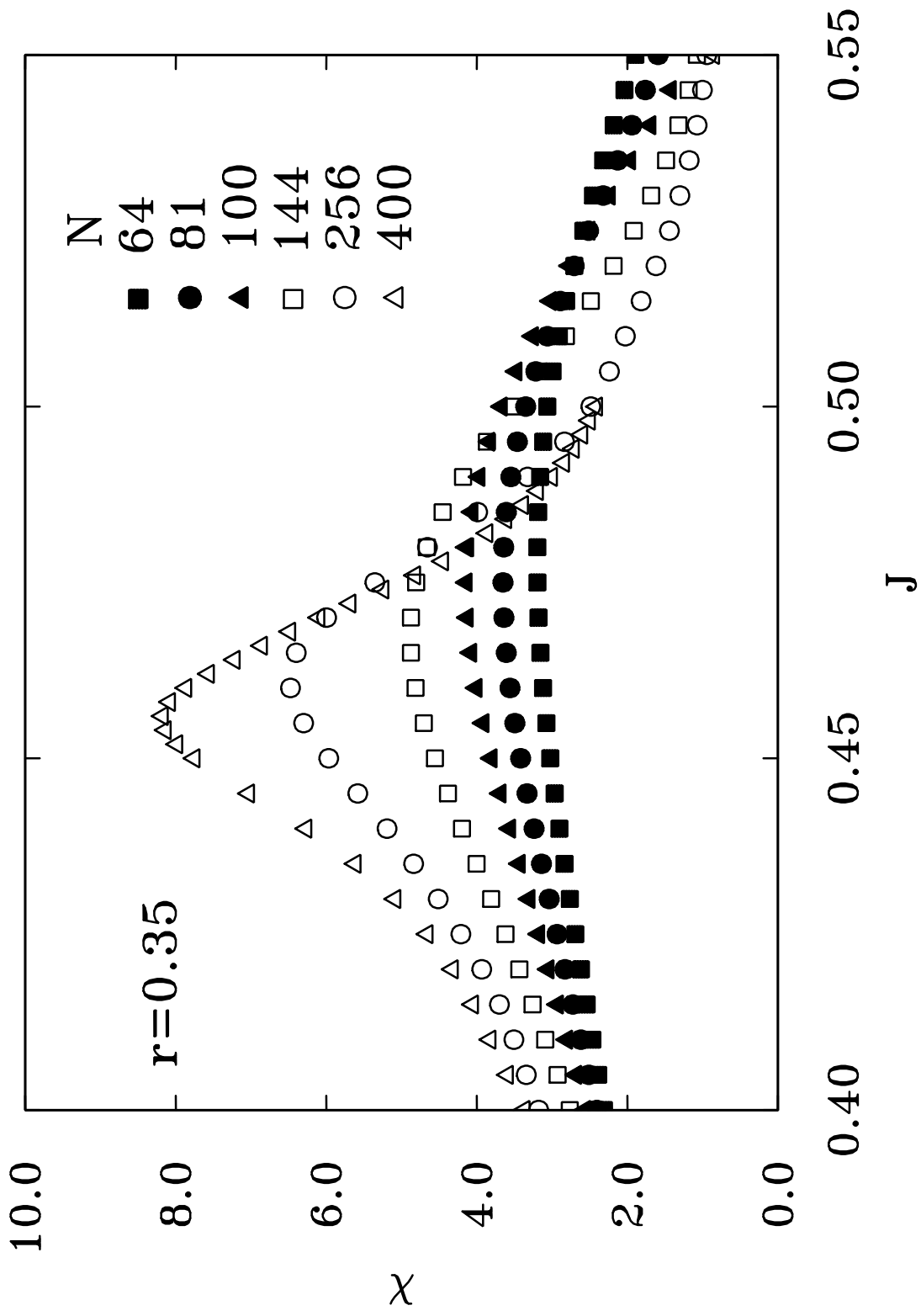


Fig.7

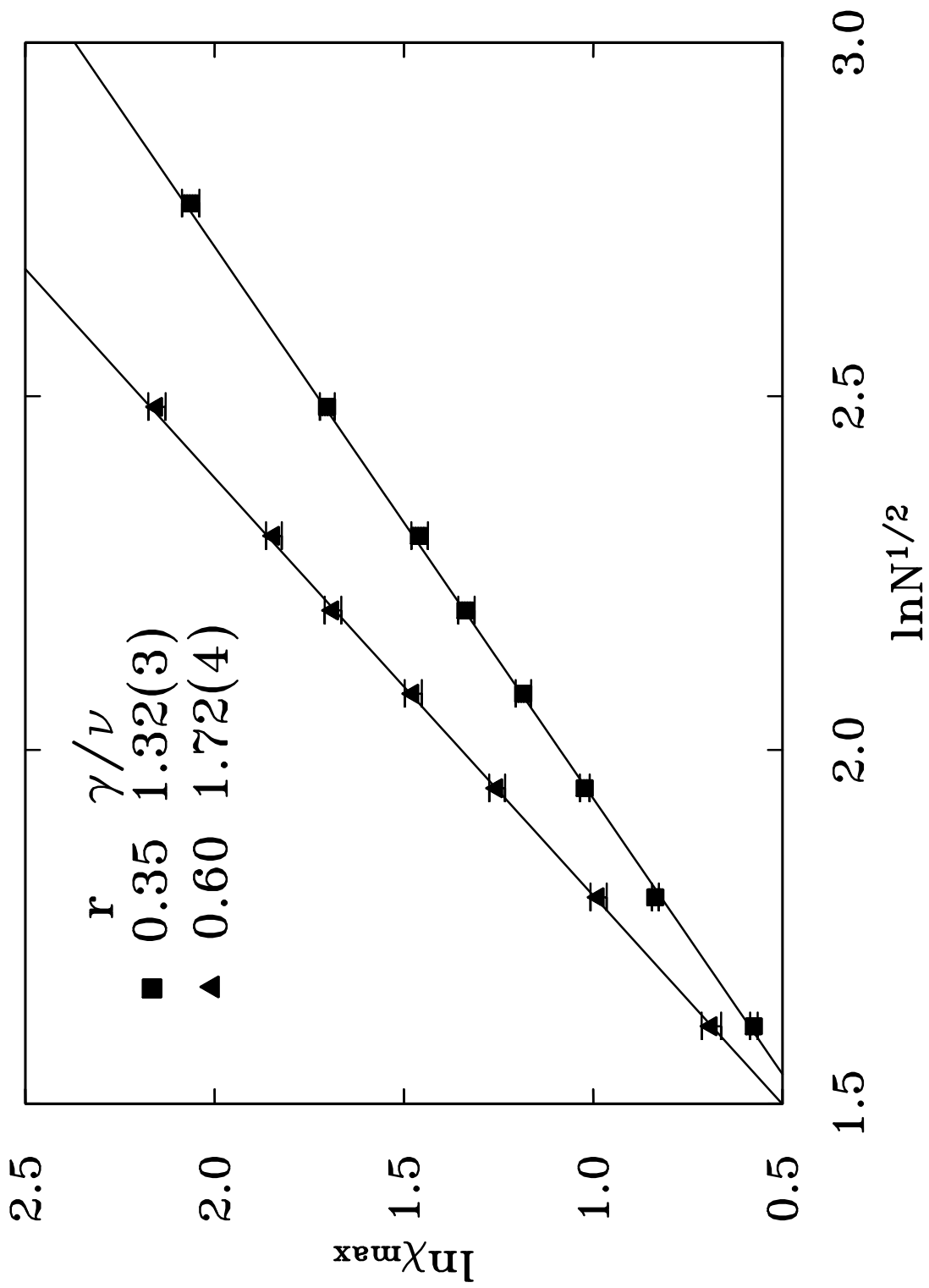


Fig.8

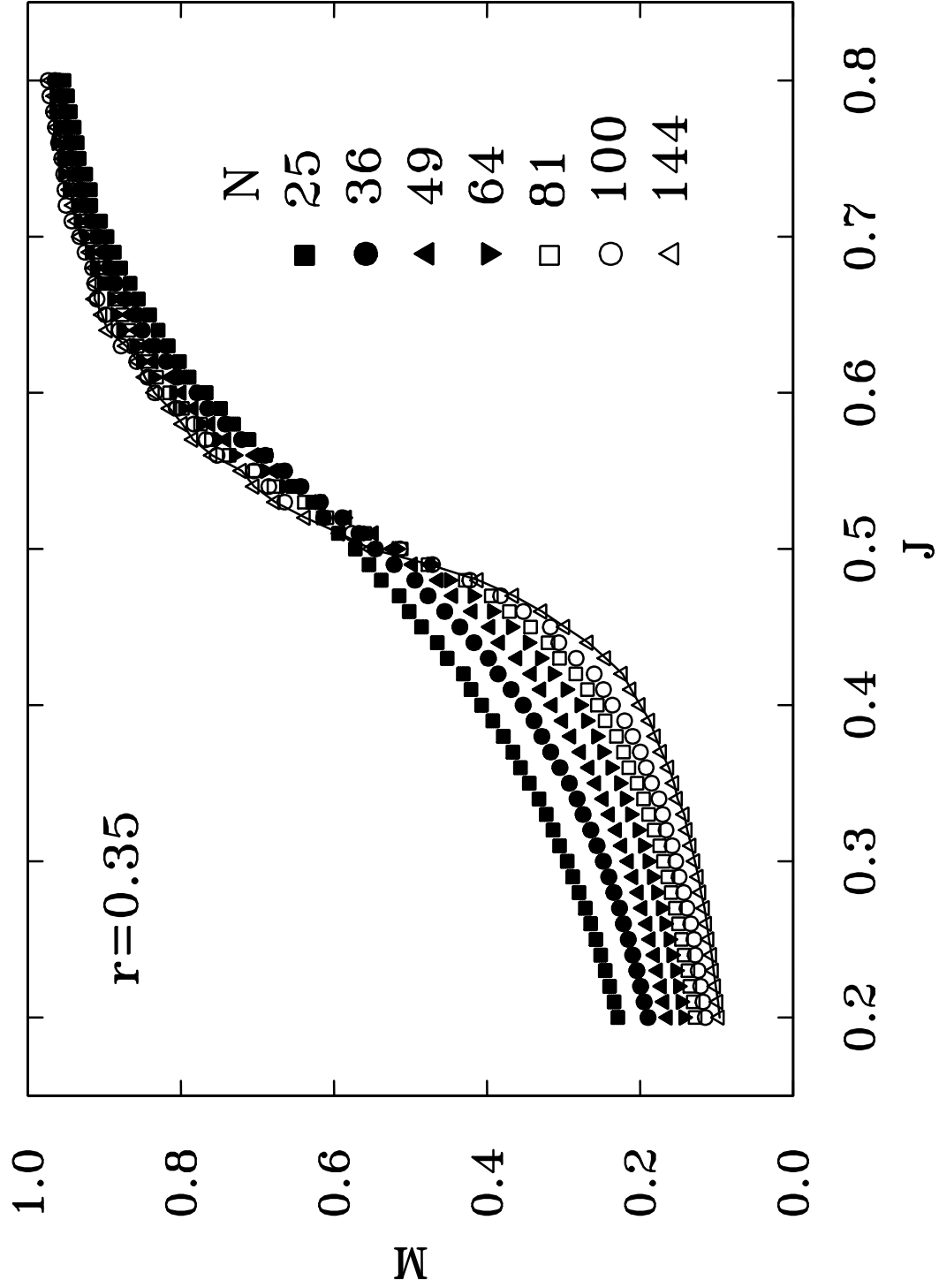


Fig.9

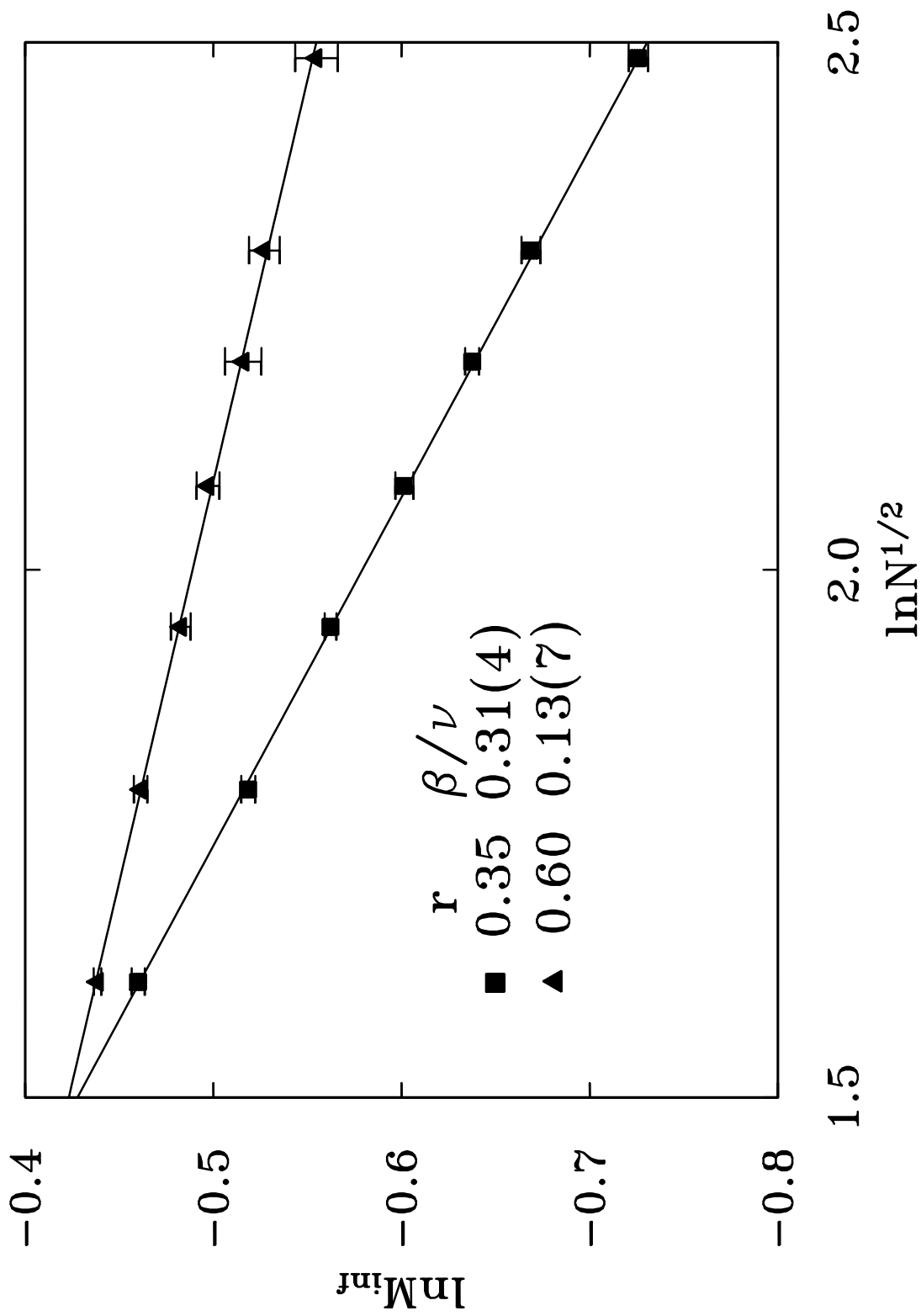


Fig.10

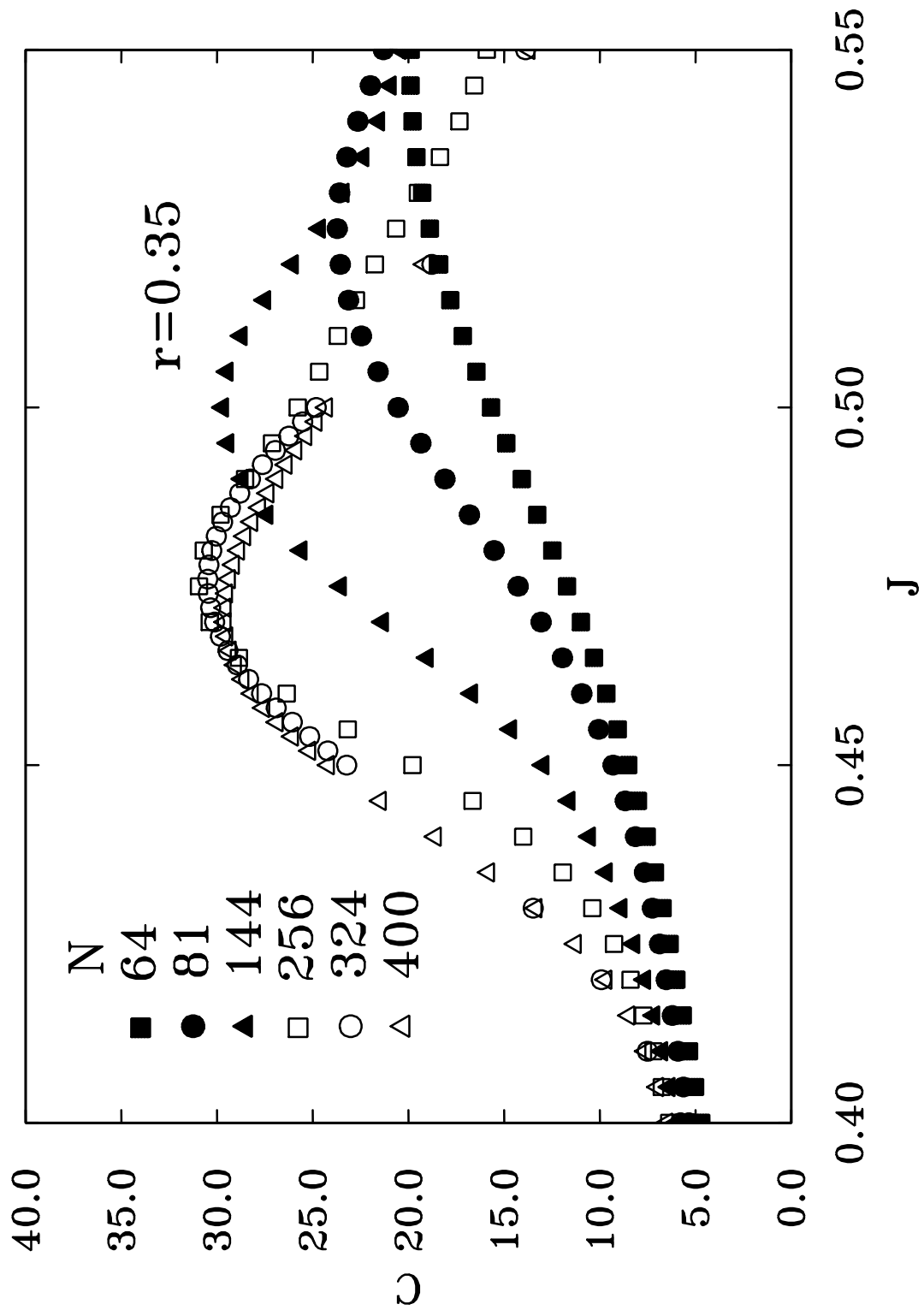


Fig.11

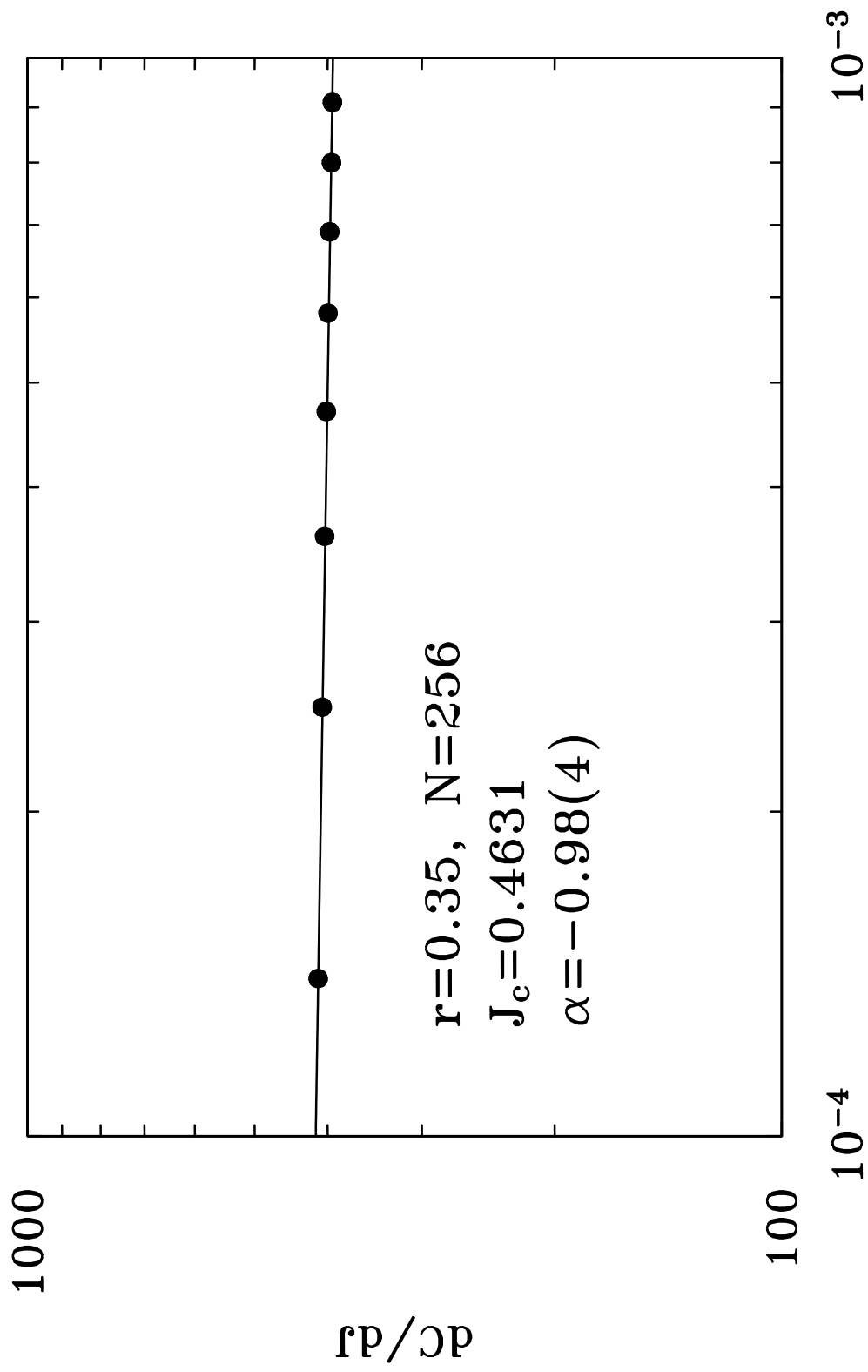
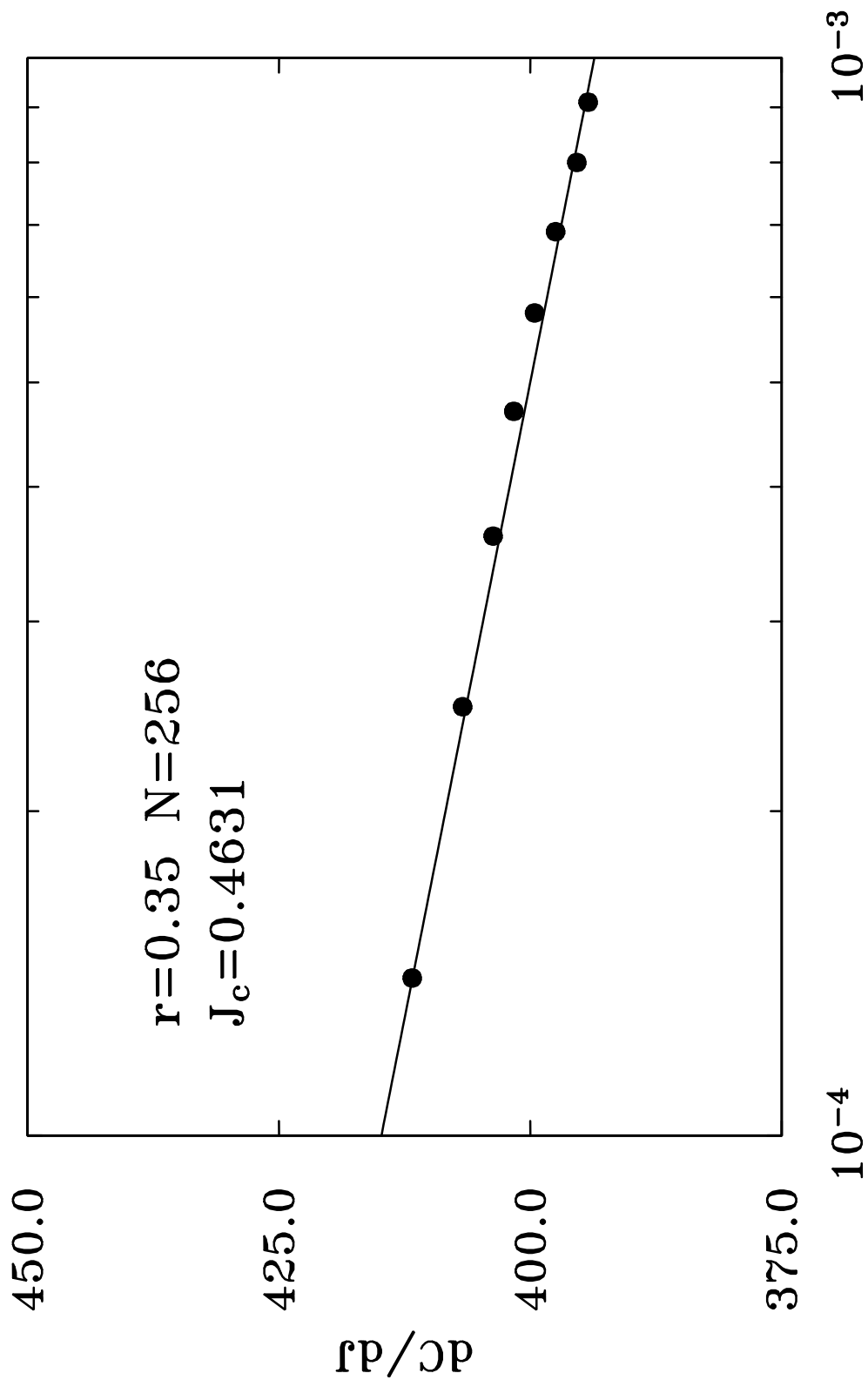


Fig.12



$J_c - J$

Fig.13

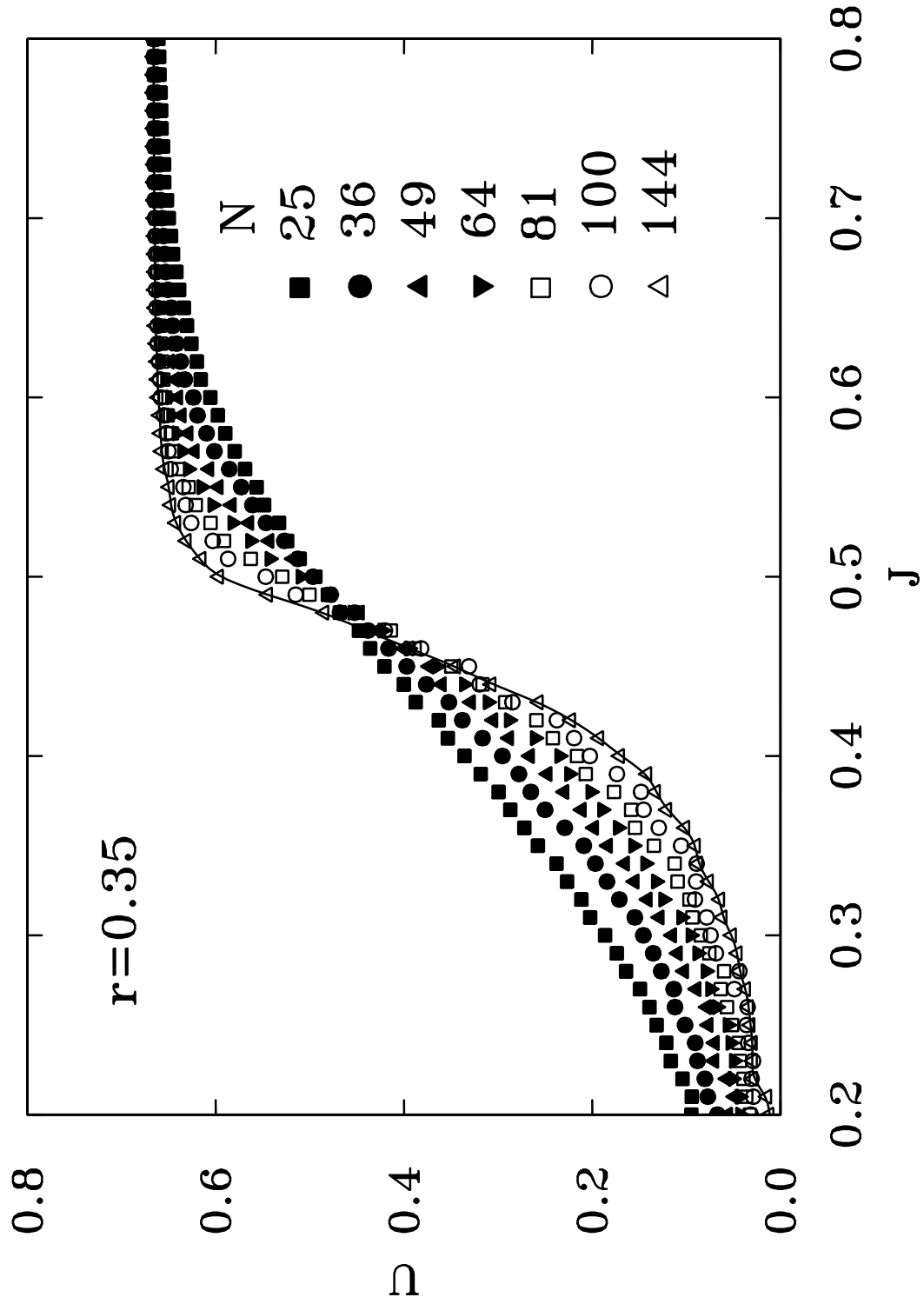


Fig.14

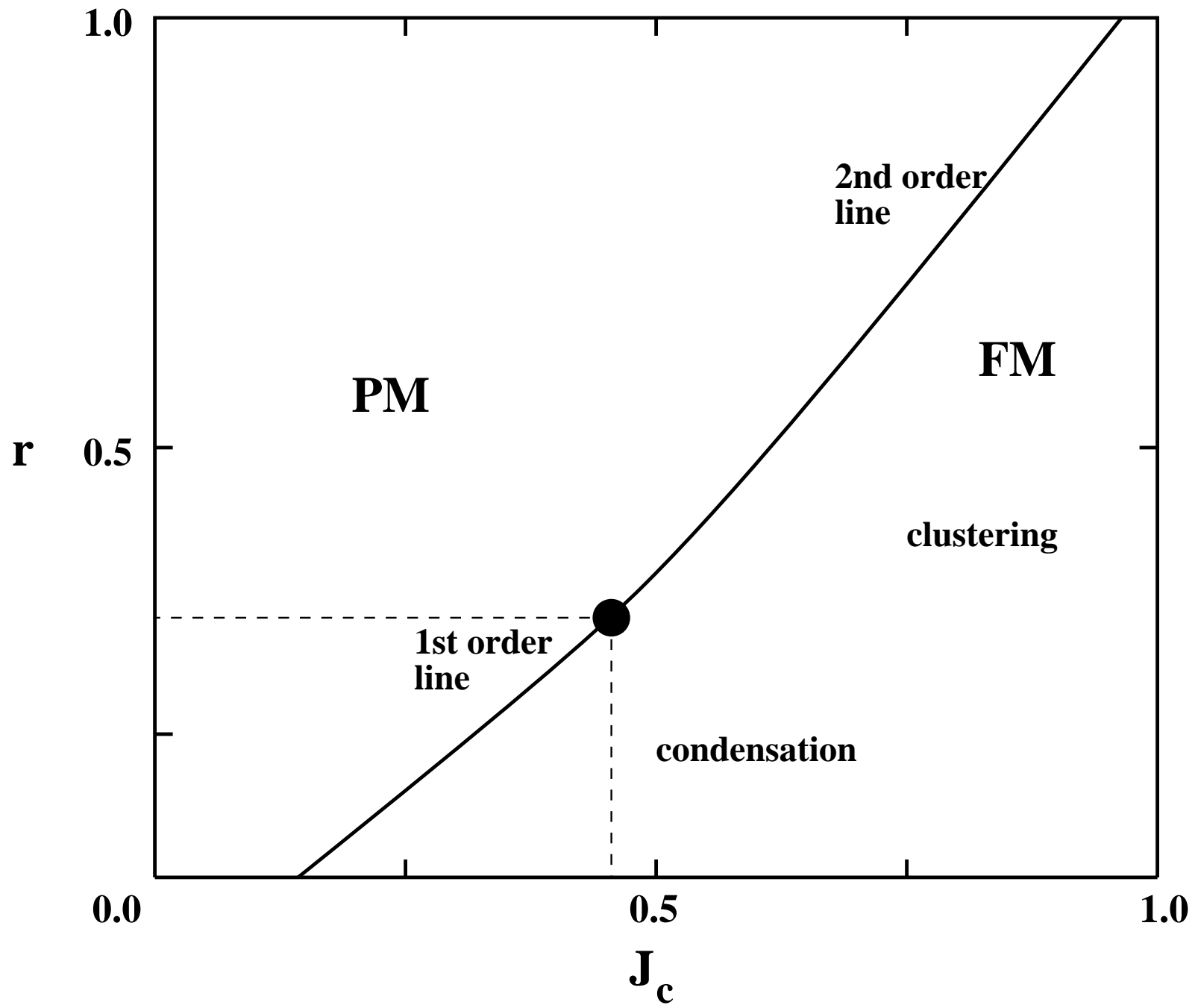


Fig.15